Mass spectrum of the $J^P = 1/2^-$ and $3/2^-$ pentaquark antidecuplets in the perturbative chiral quark model

T. Inoue, V. E. Lyubovitskij, Th. Gutsche and Amand Faessler

Institut für Theoretische Physik, Universität Tübingen, Auf der Morgenstelle 14, D-72076 Tübingen, Germany

Received (received date)
Revised (revised date)

We study the recently discovered Θ^+ baryon in the context of the perturbative chiral quark model. The basic configuration of the Θ^+ is set up as a pentaquark bound state, where the single particle wave functions are the ground state solutions of a confining potential. We classify the resulting pentaquark multiplets as the $J^P = 1/2^-$ and $3/2^-$ flavor SU(3) antidecuplet. The full mass spectrum of the multiplets is determined by including meson and gluon cloud contributions inducing flavor SU(3) breaking. Mainly due to the semi-perturbative gluon effects the resulting $3/2^-$ antidecuplet is about 185 MeV heavier than the $1/2^-$ one. We assign the observed Θ^+ baryon as a member of the $1/2^-$ antidecuplet and discuss in particular the relation to the recent experimental signal for a Ξ^{--} baryon.

1. Introduction

Recently an exotic baryon, which is now called the Θ^+, was observed by several experimental collaborations [1,2]. This baryon is supposed to be an exotic hadron with positive strangeness $S = +1$. Since such a quantum number requires the additional existence of at least a valence antiquark in the Θ^+ baryon, this minimal configuration is in clear contrast to the three valence quark picture of conventional baryons. Another characteristic property of the Θ^+ is its unusually narrow decay width. From recent experiments upper bounds for the total width of the Θ^+ were reported to be around $9 \sim 25$ MeV. Moreover, a recent revised analysis of kaon-deuteron scattering data [3] shows that the Θ^+ width should be smaller than 1 MeV if the baryon exists and if the isospin assignment equals zero. There is also an experimental (very preliminary) indication that the Θ^+ is a isosinglet [2]. After the observation of the Θ^+ another narrow exotic baryon, the Ξ^{--}, with double strangeness $S = -2$ was recently claimed to be seen [4].

Many theoretical interpretations have been put forward for the Θ^+ baryon. Originally, the Θ^+ baryon was predicted by the chiral quark soliton model [5] including its mass and narrow decay width, before it was confirmed by the experiments [1,2]. In this model baryons are considered as bound states of valence quarks in a self-consistent field of pseudoscalar mesons. The Θ^+ baryon shows up as a isosinglet member of the spin-parity multiplet $J^P = 1/2^+$ which is classified as a flavor SU(3)

antidecuplet $\bar{10}_f$. Note that the prediction of the Θ^+ baryon which is based on a collective quantization of the chiral soliton was shown to be inconsistent with large N_c QCD counting [6].

The interpretation of the Θ^+ as a quasi-bound πKN system with isospin $I = 0$ and spin-parity $J^P = 1/2^+$ was tested in Ref. [7]. The analysis in Ref. [7] is based on a solution of a partial Faddeev equation in the chiral unitary approach by assigning the κ resonance to the $K\pi$ subsystem. The authors did not obtain a bound state and concluded that the Θ^+ baryon is unlikely to be a quasi-bound πKN system.

Another popular scenario for the structure of the Θ^+ is, of course, a pentaquark picture, where the minimal configuration of four quarks and a single antiquark form a bound state. Many models for the Θ^+ baryon as a pentaquark state have been developed since the first evidence for this state was reported. They can be divided into two main categories, namely correlated [8,9] and uncorrelated quark models [10,11,12,13,14]. In the first kind of approaches strongly correlated subsystems of two or three quarks (and the antiquark) are treated as single particles. Such an ansatz leads to a considerable simplification of the inner structure of exotic baryons in terms of three- or two-body systems which is furthermore exploited.

A typical example for a correlated model is the one originally proposed by Jaffe and Wilczek [8]. They suggested that the Θ^+ baryon is a bound state of two diquarks and a single antiquark, where each diquark has spin-parity 0^+ in a $\bar{3}_c$ color and a $\bar{3}_f$ flavor state. These diquarks obey Bose statistics and their spatially antisymmetric wave function contains a P-wave in angular momentum. Exotic baryons (including the Θ^+) result from a bound system of two diquarks and a single antiquark with spin-parity either $1/2^+$ or $3/2^+$. Choosing the total spin-parity as $1/2^+$ and ideal mixing for the resulting 8_f and $\bar{10}_f$ flavor multiplets, the lightest member of the exotic multiplet is identified with the Roper resonance with a fixed mass of 1440 MeV. The parity of the Θ^+ is positive since one unit of orbital angular momentum is involved, which is compensated by the negative intrinsic parity of the antiquark.

Karliner and Lipkin considered an alternative scheme of a correlated quark model. Their approach is based on the idea that the Θ^+ baryon is considered as a bound state of a di- and a triquark [9] coupled together in a relative P-wave. The triquark is proposed to be the correlated system of two quarks and a single antiquark with total spin-parity $1/2^-$ in the 3_c, $\bar{6}_f$ state. The spin-parity of the total correlated five-quark system is $1/2^+$ and $3/2^+$ as in the Jaffe-Wilczek model. Moreover, the Θ^+ is again a member of the $\bar{10}_f$ multiplet arising from a $8_f + \bar{10}_f$ decomposition. The mass of the Θ^+ is estimated phenomenologically by using input from the D meson spectrum.

In uncorrelated quark models the five-body system is studied directly, mostly in a direct extension of the conventional baryon system consisting of three valence quarks. Several models based on different valence configurations and varieties in the residual dynamics have been proposed and studied [10,11,12,13,14]. This traditional scenario for the pentaquark structure of the Θ^+ is claimed by several authors involved

in correlated models to be problematic. In fact, because of unconstraint number of degrees of freedom the uncorrelated five-body approaches lead to a larger number of possible configurations of constituents than correlated ones. On the other hand, uncorrelated models cover a wide spectrum of possibilities for the possible pentaquark structure of the Θ^+ baryon. For example, it is possible to construct a negative parity antidecuplet within uncorrelated models, while it is difficult to be realized using the correlated approaches discussed above. The parity of the Θ^+ baryon is not experimentally determined yet. If the parity is negative, the models suggesting a positive parity for the Θ^+ baryon are ruled out immediately. In particular, QCD sum rule calculations [15,16] and a lattice QCD simulation [17] indicate a negative parity for the Θ^+. The main advantage of the five-body treatment is that the particles involved are ordinary ones, *i.e.* quarks and antiquarks, which are the same degrees of freedoms as in conventional hadrons. A straightforward extrapolation of the conventional hadron systems to their exotic partners helps to obtain a unified understanding of the complete baryon spectrum. It is relatively easy to introduce and define the dynamics in such models by assuming a universal underlying dynamical picture in explaining the full set of baryon states. Moreover, in this treatment the quark Fermi statistics can be imposed strictly, while in the correlated approaches it is only exactly fulfilled when the diquark is really a pointlike particle.

In this paper, we construct an uncorrelated pentaquark picture for the Θ^+ baryon in extension of the perturbative chiral quark model [18]. This quark model was originally developed as an effective approach to conventional baryons considered as bound states of three valence quarks which are supplemented by a cloud of pseudoscalar mesons. The model has been successfully applied to the description of canonical baryon properties [18,19,20]. In the current work, we tune the model such that it can be extended to the pentaquark systems. We then investigate the mass spectrum of the negative parity antidecuplets with spin 1/2 and 3/2, where one of the members can be associated with the Θ^+ baryon.

2. The perturbative chiral quark model (PCQM)

The perturbative chiral quark model [18,19,20] is aimed at the description of baryons based on an effective chiral Lagrangian. The model describes the valence quarks of baryons as relativistic fermions moving in an external field (static potential) $V_{\rm eff}(r) = S(r) + \gamma^0 V(r)$ with $r = |\vec{x}|$. The valence quark core is supplemented in the flavor SU(3) version by a cloud of Goldstone bosons (π, K, η) according to the chiral symmetry requirement and in addition by quantum fluctuations of the gluon field [21]. Treating also Goldstone fields as small fluctuations around the valence quark core, we derive the linearized effective chiral Lagrangian [20]:

$$\mathcal{L}_{\rm eff}(x) = \bar{\psi}(x)\left[i\,\partial\!\!\!/ - V_{\rm eff}(r)\right]\psi(x) + \frac{1}{2}\sum_{i=1}^{8}[\partial_\mu \Phi_i(x)]^2 - \frac{1}{4}F^a_{\mu\nu}F^{a\,\mu\nu}$$

$$-\bar{\psi}(x)\Big\{S(r)i\gamma^5\frac{\hat{\Phi}(x)}{F}+g_s\gamma^\mu A^a_\mu(x)\frac{\lambda^a}{2}\Big\}\psi(x)+\mathcal{L}_{\chi SB}(x) \tag{1}$$

where $F = 88$ MeV is the pion decay constant in the chiral limit[22]; g_s is the quark-gluon coupling constant; A^a_μ is the quantum component of the gluon field and $F^a_{\mu\nu}$ is its conventional field strength tensor; $\hat{\Phi} = \sum_{i=1}^{8}\Phi_i\lambda_i = \sum_P \Phi_P\lambda_P$ is the octet matrix of pseudo-scalar mesons with $P = \pi^\pm, \pi^0, K^\pm, K^0, \bar{K}^0, \eta$. The term $\mathcal{L}_{\chi SB}(x)$ in Eq. (1) contains the mass contributions both for quarks and mesons, which explicitly break chiral symmetry,

$$\mathcal{L}_{\chi SB}(x) = -\bar{\psi}(x)\mathcal{M}\psi(x) - \frac{B}{2}Tr[\hat{\Phi}^2(x)\mathcal{M}]\,. \tag{2}$$

Here, $\mathcal{M} = \mathrm{diag}\{m_u, m_d, m_s\}$ is the mass matrix of current quarks, $B = -\langle 0|\bar{u}u|0\rangle/F^2$ is the quark condensate constant. We rely on the standard picture of chiral symmetry breaking [23] and use the leading term for the masses of the pseudoscalar mesons. In our numerical calculations, we restrict to the isospin symmetry limit with $m_u = m_d = \hat{m}$. After diagonalization the physical meson masses are given by

$$M_\pi^2 = 2\hat{m}B, \qquad M_K^2 = (\hat{m}+m_s)B, \qquad M_\eta^2 = \frac{2}{3}(\hat{m}+2m_s)B\,. \tag{3}$$

In our evaluation, we choose the following set of QCD parameters [23]:

$$\hat{m} = 7\ \mathrm{MeV},\ \frac{m_s}{\hat{m}} = 25,\ B = \frac{M_{\pi^+}^2}{2\hat{m}} = 1.4\ \mathrm{GeV}. \tag{4}$$

We formulate perturbation theory in the expansion parameter $\hat{\Phi}(x)/F \sim 1/\sqrt{N_c}$ and treat finite current quark masses perturbatively [18]. All calculations are performed at one loop or at order of accuracy $o(1/F^2, \hat{m}, m_s)$.

The unperturbed eigenstates of quarks and antiquarks in the confining potential are determined by the Dirac equation

$$[i\partial\!\!\!/ - V_{\mathrm{eff}}(r)]\,\psi(x) = 0\,. \tag{5}$$

We denote the quark and the antiquark wave functions in the respective orbits α and β as:

$$u_\alpha(x) = u_\alpha(\vec{x})\exp(-i\mathcal{E}_\alpha)\,, \quad v_\beta(x) = v_\beta(\vec{x})\exp(i\mathcal{E}_\beta)\,. \tag{6}$$

The eigenstates are used for the expansion of the quark field $\psi(x)$ as

$$\psi(x) = \sum_\alpha b_\alpha u_\alpha(\vec{x})\exp(-i\mathcal{E}_\alpha t) + \sum_\beta d^\dagger_\beta v_\beta(\vec{x})\exp(i\mathcal{E}_\beta t) \tag{7}$$

where b_α and $d^\dagger_\beta$ are the corresponding single quark annihilation and antiquark creation operators.

We use the single-particle ground state configurations, namely $u_0(x)$ and $v_0(x)$, to construct the unperturbed baryonic state $|\phi_0\rangle^B$. For example, the wave function

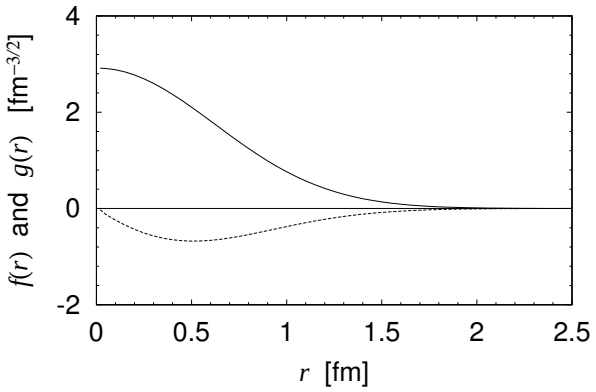

Fig. 1. Radial wave function for the valence quark: solid line for upper $g(r)$ and dashed line for lower component $f(r)$.

of conventional baryons is given by the direct product of single quark wave functions, *i.e.* by $\prod_{i=1}^{3} u_0(x_i)$ in analogy to the non-relativistic non-interacting quark model. The unperturbed wave function of the Θ^+ baryon is then set up as $\prod_{i=1}^{4} u_0(x_i)\bar{v}_0(x_5)$ in our pentaquark picture. Here, color, spin and flavor indices are suppressed. The explicit form of the ground state quark wave function is set up as

$$u_0(\vec{r}) = \begin{pmatrix} g(r) \\ -if(r)\vec{\sigma}\cdot\hat{r} \end{pmatrix} Y_0^0(\hat{r})\chi_s\chi_f\chi_c, \tag{8}$$

while for the ground state of the antiquark we have

$$v_0(\vec{r}) = \begin{pmatrix} -l(r)\vec{\sigma}\cdot\hat{r} \\ ik(r) \end{pmatrix} Y_0^0(\hat{r})\chi_s\chi_f\chi_c \ , \tag{9}$$

where in $v_0(\vec{r})$ the dominant lower component is an S-wave. The radial wave functions $f(r)$, $g(r)$, $k(r)$ and $l(r)$ are determined by the Dirac equation (5) and depend on the choice of the confining potential.

Previously we have used a three-parameter harmonic oscillator potential to set up the single-particle ground state wave functions [20]. In the present approach we generalize the confining potential to also include antiquark solutions. First we use a linear type scalar potential $S(r) = cr$ with $c = 0.11$ GeV^2. Here, the strength constant c is chosen such that the resulting quark wave functions yield a value for the charge radius of the proton with $\sqrt{< r_E^2 >_{LO}^P} = 0.76$ fm at tree level as for the harmonic case [20]. We furthermore introduce for simplicity a vector potential with $V(r) = V_0 =$ constant. A constant vector potential merely shifts the energy of the eigenstates which only appears in the absolute values of the resulting baryon

masses. For $V(r) = V_0$ the quark and antiquark wave functions are symmetric with

$$g(r) = -k(r) \quad \text{and} \quad f(r) = -l(r)\,. \tag{10}$$

Here the minus signs just occur due to our convention in defining the radial wave functions of Eqs. (8) and (9): $g(r)$ and $l(r)$ are chosen to be positive. The radial wave functions for the quark are shown in Fig. 1. The single energies of quark and antiquark are given by $\pm 537\,\mathrm{MeV} + V_0$, respectively. Previously [20] we also introduced a slight flavor dependence in the effective potential resulting in an improved fit of hyperon properties *i.e.* masses and weak decay parameters. In this paper, for simplicity, we do not introduce such a difference, hence we refer to the "symmetric parameter" version of [20].

The expectation value of an operator $\hat{A}$ in baryon B is set up as:

$$< \hat{A} >= {}^{B}\langle\phi_0| \sum_{n=0}^{\infty} \frac{i^n}{n!} \int d^4x_1 \ldots d^4x_n T[\mathcal{L}_I(x_1) \ldots \mathcal{L}_I(x_n)\hat{A}\,]|\phi_0\rangle_c^B \tag{11}$$

where $\mathcal{L}_I(x)$ refers to the interaction Lagrangian, *i.e.* the 4-th term of the total Lagrangian of Eq. (1), and subscript c refers to connected graphs only. The interaction Lagrangian includes effects of the meson cloud and gluonic quantum corrections to the baryon. For the evaluation of Eq. (11) we apply Wick's theorem with appropriate propagators for quarks, mesons and gluons.

For the quark field we use a Feynman propagator for a fermion in a binding potential with

$$iG_\psi(x,y) = \langle 0|T\{\psi(x)\bar{\psi}(y)\}|0\rangle \tag{12}$$

and

$$\begin{aligned} iG_\psi(x,y) = {} & \theta(x_0 - y_0) \sum_\alpha u_\alpha(\vec{x})\, \bar{u}_\alpha(\vec{y})\, e^{-i\mathcal{E}_\alpha(x_0 - y_0)} \\ & - \theta(y_0 - x_0) \sum_\beta v_\beta(\vec{x})\, \bar{v}_\beta(\vec{y})\, e^{i\mathcal{E}_\beta(x_0 - y_0)}\,. \end{aligned} \tag{13}$$

In the present study we restrict the expansion of the quark propagator to the ground state both for quarks and antiquarks. For the meson fields we adopt the free Feynman propagator with

$$i\Delta_{PP'}(x-y) = \langle 0|T\{\Phi_P(x)\Phi_{P'}(y)\}|0\rangle = \delta_{PP'} \int \frac{d^4k}{(2\pi)^4 i} \frac{\exp[-ik(x-y)]}{M_P^2 - k^2 - i\epsilon}. \tag{14}$$

For the gluon field we use the dressed propagator containing an effective quark-gluon coupling constant $\alpha_s(k^2) = g_s^2(k^2)/(4\pi)$ with a nontrivial momentum dependence. In our considerations we work in Coulomb gauge to separate the contributions of Coulomb (A_0^a) and transverse (A_i^a) gluons in the propagator:

$$i\,\alpha_s\, D_{00}^{ab}(x-y) \;=\; -\,\delta^{ab} \int \frac{d^4k}{(2\pi)^4 i} \frac{e^{-ik(x-y)}}{\vec{k}^{\,2}}\, \alpha_s(k^2) \tag{15}$$

and

$$i\,\alpha_s\,D^{ab}_{ij}(x-y)\;=\;\delta^{ab}\int\frac{d^4k}{(2\pi)^4 i}\frac{e^{-ik(x-y)}}{k^2+i\varepsilon}\left\{\delta_{ij}-\frac{k_i k_j}{\vec{k}^{\,2}}\right\}\alpha_s(k^2)\,. \tag{16}$$

Following an approach to low-energy QCD as based on the solutions of the Dyson-Schwinger equations [24] we suppose that the running coupling constant $\alpha_s(k^2)$ includes nontrivial effects of vertex and self-energy corrections, etc. In the present paper we use a simple analytic form for α_s as suggested in Ref. [24]:

$$\alpha_s(t)\;=\;\frac{\pi}{\omega^6}Dt^2e^{-t/\omega^2}+\frac{2\gamma_m\pi}{\ln\left[\tau+\left(1+t/\Lambda^2_{QCD}\right)^2\right]}F(t) \tag{17}$$

where $t=-k^2$ is an Euclidean momentum squared, $F(t)=1-\exp(-t/[4m_t^2])$, $\tau=e^2-1$, $\gamma_m=12/(33-2N_f)$, $\Lambda^{N_f=4}_{QCD}=0.234$ GeV, $\omega=0.3$ GeV and $m_t=0.5$ GeV. The functional form of $\alpha_s(t)$ was fitted to the perturbative QCD result in the ultraviolet region (at large momentum squared) and is governed by a single parameter D in the infrared region. In Ref. [24] the parameter $D=(0.884\,\mathrm{GeV})^2$ was adjusted phenomenologically to reproduce properties of pions and kaons described as bound states of constituent quarks. In our considerations we fit the effective coupling with $D=(0.5\,\mathrm{GeV})^2$ such that the $\Delta-N$ mass splitting is reproduced [20]. The running coupling $\alpha_s(t)$ between quarks and gluons should be considered as effective, since it depends on the way its used in phenomenology. Since in our model we utilize gluon as well as meson degrees of freedom, it is natural that our fitted value for D is smaller than the one of Ref. [24]. Namely, the relatively small value for D leaves space for meson cloud effects in the infrared region.

3. Pentaquark baryon systems and mass spectrum

The pentaquark baryon systems include a four-quark subsystem which is totally antisymmetric under the permutation of quarks. We begin with the discussion of this subsystem. In the context of a potential model, where the residual interaction is treated perturbatively, it is natural to start with the energetically favored configuration where all four quarks are in the ground state orbit. Some models [11,13] discuss a configuration with an excited quark which is the energetically lowest one. However, the issue of level reversing in the basic five-quark configuration strongly depends on the dynamics involved in the model. In the context of our model we assume no excitation for the beginning. We will return to this point later on. With this condition the four-quark subsystem is symmetric in orbital space and in a color 3_c state such that the total pentaquark system is a color singlet; hence the subsystem is mixed symmetric in color space. The Θ pentaquark includes four u and d quarks. The spin and isospin coupling of the four non-strange quarks can in general result in total spin S=0,1,2 and isospin I=0,1,2. The (S=2, I=2) state is forbidden here, since both the S=2 and I=2 configurations are symmetric in the respective space and a totally antisymmetric four-quark subsystem cannot be formed, when

combined with the orbital and color symmetries. The possible spin-isospin combinations which result in a totally antisymmetric configuration are (S=0, I=1), (S=1, I=0), (S=1, I=2) and (S=2, I=1) [25].

Capstick *et al.* studied the (S=1, I=2) combination [10]. In this model the Θ^+ baryon is a member of a isotensor multiplet: $\{\Theta^{+++}, \Theta^{++}, \Theta^{+}, \Theta^{0}, \Theta^{-}\}$ and its narrow decay width is explained by isospin conservation. Carlson *et al.* originally studied the case of (S=1, I=0) [12]. Yet the authors revised their work by referring to a configuration with one orbital excitation, in line with their estimate of the energy-shift due to the specific residual interaction [13]. There is experimental indication that the Θ^+ baryon seems to be an isoscalar [2]. We follow this suggestion and choose the (S=1, I=0) combination in our considerations. All four-quark combinations exist simultaneously in the present quark model, and each of these will correspond to a certain baryon multiplet. A complete case for pentaquarks should be able to put forward a consistent dynamical mechanism to explain the observable part of these multiplets and the decay characteristics of the experimentally accessible states. We will comment on this point later on.

The isosinglet four-quark combination with the [**22**] Young tableau in the two-flavor picture becomes the $\bar{6}_f$ in the flavor SU(3) generalization. Therefore, by adding a single antiquark ($\bar{3}_f$) to the four-quark system we generate pentaquark states which split into the 8_f and the $\bar{10}_f$ flavor SU(3) multiplets as in the Jaffe-Wilczek [8] and Karliner-Lipkin [9] models. The Θ^+ baryon then belongs to the antidecuplet $\bar{10}_f$.

The spin-parity of the four-quark subsystem with (S=1, I=0) is 1^+. In the context of the model it is natural to assume that the antiquark is also in a S-wave ground state. As a consequence the spin-parity of the pentaquark states are $1/2^-$ and $3/2^-$, where, since no angular-momentum excitations are introduced, the parity is negative. This point is characteristic of the present approach when compared to other models (see discussion in Section 1). In total we have 36 pentaquark states distributed among four multiplets: two octets and two antidecuplets with two possible spin-parities, $1/2^-$ and $3/2^-$. Their explicit wave functions can, for example, be constructed by dividing the four-quark subsystem into two-quark pairs (for a detailed discussion see Ref. [12]).

In the following we restrict the application of the PCQM to the study of the mass spectrum of the negative parity antidecuplet $\bar{10}_f$. In the isospin symmetry limit we consider the masses of the Θ, N, Σ and Ξ baryons denoting the isospin multiplets in each row of the antidecuplet. At this point we do not introduce a mixing between the 8_f and the $\bar{10}_f$. The resulting masses of N and Σ may therefore not correspond to physical ones even if the present approach is realistic. If and how strong the ensuing mixing develops dynamically is currently an open issue. The masses of the Θ and the Ξ are not affected by this mixing. We consider both the spin 1/2 and 3/2 antidecuplets and study the mass splittings, in particular of Θ and Ξ, induced by the flavor dependent current quark masses and by residual interactions.

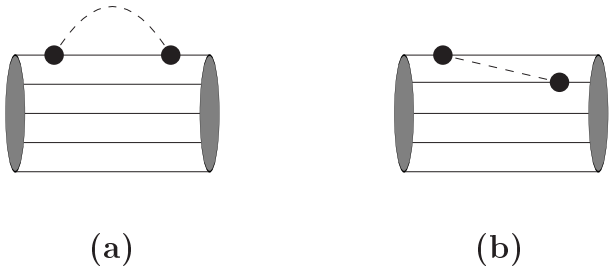

Fig. 2. Meson loop diagrams contributing to the pentaquark energy shift: meson cloud (2a) and exchange diagrams (2b).

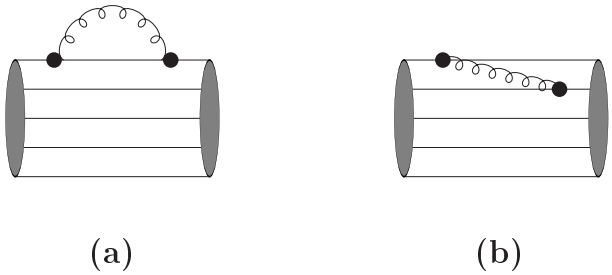

Fig. 3. Gluon loop diagrams contributing to the pentaquark energy shift: gluon cloud (3a) and exchange diagrams (3b).

First, on the level of the model confinement the exotic baryon masses of the four different isomultiplets develop mass differences due to the different strange quark/antiquark content including the hidden one. In the present approach finite current quark masses contribute a linear term with $\sum_{i=1}^{5} m_i\gamma$ to the baryon mass, where $\gamma = \int d^3x\, \bar{u}_0(x)u_0(x)$ is the relativistic reduction factor[18]. For the number of valence quarks, that is nonstrange (n) and strange quarks (s) and similarly for the antiquarks ($\bar{n}$ and $\bar{s}$) in each baryon, one can use the numbers listed in Table 14 of the Appendix. In the current model the total number of s plus $\bar{s}$ is one unit larger in Ξ than in Θ as is known from Ref. [12,26].

Second, the residual quark interaction induces energy shifts depending on the particular pentaquark state. In the PCQM the energy shift of the pentaquark valence particles interacting with pseudoscalar mesons and quantum gluon fields is evaluated perturbatively as

$$\Delta m_B = {}^B\langle\phi_0| \sum_{n=1}^{2} \frac{i^n}{n!} \int i\delta(t_1) d^4x_1 \ldots d^4x_n T[\mathcal{L}_I(x_1)\ldots\mathcal{L}_I(x_n)]|\phi_0\rangle_c^B \qquad (18)$$

where $\mathcal{L}_I(x)$ is the interaction Lagrangian set up in Eq. (1). The resulting diagrams

contained in Δm_B are shown in Fig. 2 (meson contribution) and in Fig. 3 (gluon contribution) where the five internal solid lines represent both the valence quarks and antiquark. For example, the contribution of pion-exchange between two quarks to the pentaquark mass shift is given by

$$\Delta m_B^{\pi-\mathrm{EX};qq} = -\frac{1}{6\pi^2 F^2}\int_0^\infty dk\,\frac{k^2\,G^2_{\pi qq}(k^2)}{M_\pi^2+k^2}\,\langle B|\sum_{i<j}^{4}\sum_{a=1}^{3}\lambda_i^{(a)}\lambda_j^{(a)}\,\vec{\sigma}_i\cdot\vec{\sigma}_j\;|B\rangle\,, \qquad (19)$$

where $G_{\pi qq}(k^2)$ is the πqq coupling form factor given by:

$$G_{\pi qq}(k^2) = \int_0^\infty dr\,r^2\,[2f(r)g(r)]\,S(r)j_1(kr)\;. \qquad (20)$$

Similarly, the contribution of pion-exchange, now between a quark and an antiquark, is

$$\Delta m_B^{\pi-\mathrm{EX};q\bar{q}} = -\frac{1}{6\pi^2 F^2}\int_0^\infty dk\,\frac{k^2\,G_{\pi qq}(k^2)G_{\pi\bar{q}\bar{q}}(k^2)}{M_\pi^2+k^2}\,\langle B|\sum_{i=1}^{4}\sum_{a=1}^{3}\lambda_i^{(a)}\lambda_5^{(a)}\,\vec{\sigma}_i\cdot\vec{\sigma}_5\;|B\rangle \qquad (21)$$

where index "5" refers to the antiquark. The form factor $G_{\pi\bar{q}\bar{q}}(k^2)$ describing the coupling of a π-meson to two antiquarks is expressed by the components of the antiquark wave function $v_0(\vec{r})$:

$$G_{\pi\bar{q}\bar{q}}(k^2) = \int_0^\infty dr\,r^2\,[2k(r)l(r)]\,S(r)j_1(kr)\;. \qquad (22)$$

The contribution of gluon exchange between two quarks to the pentaquark mass shift is

$$\begin{aligned}\Delta m_B^{\mathrm{gl}-\mathrm{EX};qq} &= \frac{1}{2\pi}\int_0^\infty dk\,\alpha_s(k^2)\,G_E^2(k^2)\,\langle B|\sum_{i<j}^{4}\vec{\lambda}_i^C\cdot\vec{\lambda}_j^C\;|B\rangle \\ &\quad -\frac{1}{3\pi}\int_0^\infty dk\,\alpha_s(k^2)\,G_M^2(k^2)\,\langle B|\sum_{i<j}^{4}\vec{\lambda}_i^C\cdot\vec{\lambda}_j^C\,\vec{\sigma}_i\cdot\vec{\sigma}_j\;|B\rangle \qquad (23)\end{aligned}$$

where the first and second terms arise from the electric and magnetic contribution, respectively. The corresponding form factors $G_E(k^2)$ and $G_M(k^2)$ are defined by

$$G_E(k^2) = \int_0^\infty dr\,r^2\,\left[f^2(r)+g^2(r)\right]\,j_0(kr) \qquad (24)$$

$$G_M(k^2) = \int_0^\infty dr\,r^2\,[2f(r)g(r)]\,j_1(kr), \qquad (25)$$

where $\alpha_s(k^2)$ is the running quark-gluon coupling constant (see Section 2).

Table 1. Mass shifts of the spin 1/2 antidecuplet baryons in units of MeV.

	quark mass	meson	gluon
Θ	148	−429	−603
N	189	−399	−603
Σ	230	−367	−603
Ξ	271	−333	−603

Table 2. Mass shifts of the spin 3/2 antidecuplet baryons in units of MeV.

	quark mass	meson	gluon
Θ	148	−450	−397
N	189	−423	−397
Σ	230	−397	−397
Ξ	271	−373	−397

The contribution of all other occurring diagrams can be given in a similar fashion. We omit so called Z-type self-energy Feynman diagrams to avoid possible double counting. All relevant flavor-spin and color-spin matrix elements are summarized in the Appendix.

Numerical values for the mass shifts of the pentaquark states are deduced for our specific confining trial potential. In Tables 1 and 2 we summarize the results for the mass shifts of the spin 1/2 and 3/2 antidecuplet baryons, respectively. Column "quark mass" refers to the mass shifts induced by the current quark mass. Including relativistic effects the current quark mass induces 41 MeV splittings between consecutive rows of the antidecuplet. Therefore, because of the quark mass term the Ξ becomes 123 MeV heavier than the Θ, which is a typical result of pentaquark models.

The meson cloud leads to a considerable lowering of the antidecuplet baryon masses of about 400 MeV. This value is larger than for the case of conventional baryons of about 300 MeV. SU(3) flavor symmetry breaking as induced by the flavor dependent meson masses has qualitatively the same effect as for the case of the current quark mass. The respective splittings lead to an increase in mass when descending in the rows of the multiplet. For example, the Ξ becomes heavier than the Θ^+ by 96 MeV in the spin 1/2 antidecuplet, and by 86 MeV in the spin 3/2 antidecuplet. The negative mass shift due to the meson cloud is stronger in the spin 3/2 antidecuplet than in the spin 1/2 one. The difference arises from the exchange contribution between the quarks and the antiquark. This particular contribution is included in some studies [12], while omitted in others [14]. It is repulsive in the total spin 1/2 channel and attractive for the spin 3/2 pentaquark baryons (see Tables 5

and 6 in the Appendix). Therefore, a residual quark interaction solely based on a mesonic mechanism leads to spin 3/2 pentaquark baryons which are lighter than the flavor partners of the spin 1/2 one. But in our model the size of the splitting is not so large, about $20 \sim 40$ MeV. For the usual ground state baryons consisting of three valence quarks, meson cloud effects lead in the present model to a spin 3/2 decuplet which is about 100 MeV heavier than the spin 1/2 octet [20].

The applied semi-perturbative gluon mechanism splits the two spin states by 206 MeV, such that the spin 3/2 antidecuplet is heavier than the spin 1/2 one. This feature is quite similar to that of the ground state spin 1/2 and 3/2 case, where three valence quarks are involved. The origin of the splitting is traced to the magnetic part of the exchange contribution between the quarks and the antiquark. For the spin 1/2 pentaquark baryon it is attractive while for spin 3/2 it is repulsive (see Tables 7 and 8 in the Appendix). Here, we use the same dressed gluon propagator for the exchange between two quarks, and also between a quark and an antiquark. The results we obtain for the gluon induced mass shifts are qualitatively consistent with Ref.[14].

Within the hybrid mechanism of the present model, the spin 3/2 antidecuplet baryons become in total heavier than the spin 1/2 one. Within this context the observed Θ^+ is likely to be assigned to the lighter spin 1/2 multiplet. The splitting of about 185 MeV, however, is not so large. As a consequence of the present scenario the spin 3/2 Θ baryon is located at 1725 MeV. The negative parity spin 1/2 Θ at around 1540 MeV can decay to the S-wave KN system, while for spin 3/2 the Θ baryon cannot. In this scenario we still need to account for the observed narrow decay width of the Θ baryon. The reduced overlap between the decay channel KN and the Θ resonance with the present color-spin-flavor wave function provides a suppression of the decay width by a factor 1/4 [12]. This can explain part of the weak coupling to the KN channel.

The mass difference between the Θ and the Ξ in the spin 1/2 antidecuplet is 220 MeV in total. Using a Θ mass of 1540 MeV as input the model predicts a spin 1/2 Ξ baryon with negative parity at around 1760 MeV. This result is 100 MeV lower than the recent experimental finding for a Ξ^{--} at about 1860 MeV [4]. In the present study we have used a simplified confinement model leading to symmetric quarks/antiquark wave functions. The discrepancy may indicate that a more realistic confinement is needed. At least in the context of the mass spectrum the two possibly observed Θ^+ and Ξ^{--} baryons can be associated with members of the 1/2 multiplet. In the present model effects of flavor symmetry breaking work constructively and lead to considerable splitting between these two states. A discussion of only the mass spectrum is obviously not sufficient to judge the nature of the observed exotic baryon states. In particular, experimental information on parity and spin of both states is urgently needed to constrain and also select the theoretical approaches.

In the present simple model the energy of an unperturbed single quark or antiquark in the ground state orbit is $537\,\mathrm{MeV} \pm V_0$, respectively, where V_0 is the

Table 3. Antidecuplet pentaquark masses in units of MeV.

	Θ	N	Σ	Ξ
$J^P = 1/2^-$	1540	1611	1684	1759
$J^P = 3/2^-$	1725	1793	1860	1925

value of the constant vector potential (see Section 2). Starting from this independent particle model the unperturbed mass of the pentaquark system is given by $2685\,\mathrm{MeV} + 3V_0 - E_{\mathrm{cm}}^{5\mathrm{q}}$, where $E_{\mathrm{cm}}^{5\mathrm{q}}$ represents the spurious energy of the center-of-mass motion. By simply setting $3V_0 - E_{\mathrm{cm}}^{5\mathrm{q}} = -261$ MeV and using in addition the obtained total mass shift of -884 MeV for the spin 1/2 Θ, we fit the mass of the Θ^+ baryon of 1540 MeV. Similarly, the unperturbed mass of the three-quark system is given by $1611\,\mathrm{MeV} + 3V_0 - E_{\mathrm{cm}}^{3\mathrm{q}}$, and in this case the nucleon mass can be fitted as well. The two spurious energies $E_{\mathrm{cm}}^{3\mathrm{q}}$ and $E_{\mathrm{cm}}^{5\mathrm{q}}$ are in general different (judging from the non-relativistic harmonic oscillator potential $E_{\mathrm{cm}}^{5\mathrm{q}}$ should be smaller than $E_{\mathrm{cm}}^{3\mathrm{q}}$), hence the mass difference between the nucleon and the Θ^+ cannot be predicted in the present approach. The obtained mass spectrum of antidecuplet pentaquarks is indicated in Table3.

Finally, we give indications for the validity of our basic model configuration, where all valence quarks and the antiquark are placed in ground state orbits with the four-quark coupling (S=1, T=0). In the work by Carlson *et al.* [13] it is shown that a configuration with one excited quark is energetically favored to the one without, despite the additional excitation energy under the influence of the spin-isospin dependent interquark force. This is not the case in our model although we also have a spin-isospin force induced by one-pion exchange. In Ref. [13] the strength of this force is chosen such to reproduce the full N-Δ splitting, and is about 3 times stronger than in our case. When repeating their calculation with a reduced force by a factor of 1/3, the levels do not reverse anymore. Hence, the level reversing found in Ref. [13] does not pose a problem in the current model context.

At present it is certainly worthwhile to consider other basic pentaquark configurations (such as the I=1 four-quark combination and also the ones including single particle excitations) to obtain the full mass spectra of these systems. Mixing between these configurations and coupling to the decay channels furthermore complicate this issue. Again, a clear dynamical argument should be finally developed to work out the observable part of the pentaquark spectra in close relation to present and future experimental findings.

4. Θ^+ baryon decay width

In this Section we discuss a possible mechanism for a small decay width of the Θ^+ baryon in the framework of PCQM using an uncorrelated five-quark configuration for pentaquarks. Different models have been applied to explain an extremely small

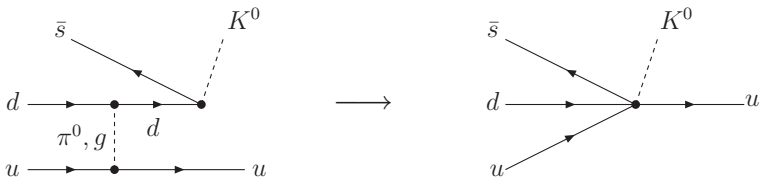

Fig. 4. Possible mechanism to generate effective coupling $K^0\bar{s}uud$.

width of Γ_{Θ^+} for the Θ^+ baryon (see detailed discussion in recent papers [27,28,29]). The current experimental status of the Θ^+ width as follows. Several recent experiments give upper limits in range 1-4 MeV [28]. The experiment on K^+ collisions on xenon and deuterium gives smaller value of $\Gamma_{\Theta^+} = 0.9 \pm 0.3$ MeV [27]. Below we derive the expression for width of $\Theta^+(\frac{1}{2}^-)$ baryon in terms of unknown coupling of the kaon to the strange antiquark and three nonstrange quarks. Next we estimate this coupling using our formalism.

To generate a connected Feynman diagram describing the transition $\Theta^+ \to p(n) + K^0(K^+)$ we need a coupling of the kaon to the strange antiquark and three nonstrange quarks: $K^0\bar{s}uud$ for the decay into the proton and $K^+\bar{s}udd$ for the decay into the neutron. In the framework of the constituent quark model this vertex can be understood as an effective coupling generated in second order of perturbation theory (for example, due to the exchange by a neutral pion or gluon). Therefore, we suggest that the transition $\Theta^+ \to p(n) + K^0(K^+)$ is governed by a higher-order operator which probably explains the small width of the Θ^+ baryon. We understand that this scenario is not unique and a more detailed study of the problem should be done, but it goes beyond the current manuscript. In Fig. 4 we draw a possible second-order diagram (left panel) generating the effective $K^0\bar{s}uud$ coupling which is a part of the effective local Lagrangian

$$\mathcal{L}_{Kq^4}(x) = -\frac{c_{Kq^4}}{F^3}\bar{K}^0(x)\bar{u}(x)\Gamma_1 u(x)\bar{s}(x)\Gamma_2 d(x) + \text{h.c.} \tag{26}$$

where c_{Kq^4} is an unknown dimensionless coupling constant; Γ_1 and Γ_2 are the Dirac spin matrices. The coupling $K^+\bar{s}udd$ (diagram and effective Lagrangian) can be obtained via the replacements $u \leftrightarrow d$ and $K^0 \to K^+$. We choose the simplest set of possible spin matrices in the Lagrangian (26): $\Gamma_1 = I$ and $\Gamma_2 = i\gamma_5$. The effective coupling $g_{\Theta NK}$ for the negative-parity pentaquark is defined as

$$\mathcal{L}_{\Theta NK}(x) \,=\, i\, g_{\Theta NK}\, \bar{N}(x)\, \Theta^+(x)\, K(x) \,+\, \text{h.c.} \tag{27}$$

where N and K are the doublets of nucleons (p, n) and kaons (K^0, K^+), respectively. A straightforward calculation of $g_{\Theta NK}$ in the PCQM relates it to c_{Kq^4}:

$$g_{\Theta NK} \,=\, \frac{1}{32\pi^2}\,\frac{c_{Kq^4}}{F^3}\,\int d^3x\,[g^2(x) - f^2(x)]\,[g^2(x) + f^2(x)] \tag{28}$$

where g and f are the components of the ground-state quark wave function (8). On

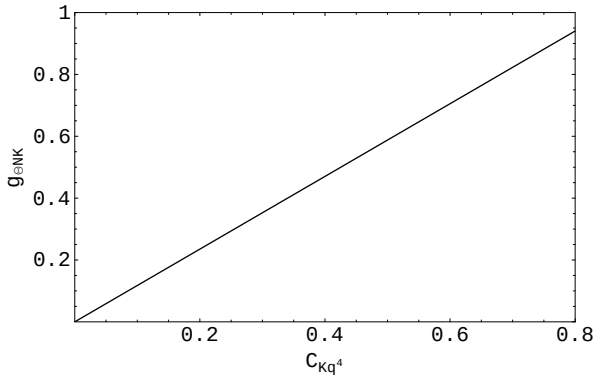

Fig. 5. Coupling $g_{\Theta NK}$ as function of c_{Kq^4}.

the other hand, $g_{\Theta NK}$ is related to the Θ^+ width as [28]

$$\Gamma_{\Theta^+} = \frac{g^2_{\Theta NK}}{8\pi m^3_\Theta}\,\lambda^{1/2}(m^2_\Theta, m^2_N, M^2_K)\,[(m_\Theta + m_N)^2 - M^2_K] \tag{29}$$

where $\lambda(x,y,z) = x^2 + y^2 + z^2 - 2xy - 2yz - 2xz$ is the Källen triangle function. In Figs. 5 and 6 we demonstrate the behavior of the quantities $g_{\Theta NK}$ and Γ_{Θ^+} as functions of effective constant c_{Kq^4}. Note, that the central value of $\Gamma_{\Theta^+} = 0.9 \pm 0.3$ MeV [27] corresponds to $c_{Kq^4} = 0.12$. Using our formalism we can estimate the coupling c_{Kq^4} relying on the idea that the two-body forces between nonstrange quarks are generated by the one-pion exchange (see left panel in Fig.4). Our result is: $c_{Kq^4} = 0.33$. It gives $\Gamma_{\Theta^+} = 7$ MeV which overestimates the current upper limits for this quantity [27]. Other possibilities for the negative-parity Θ^+ pentaquark to have a small width is also discussed in the content of other theoretical approaches (see, for example, discussion in Refs. [28,30]).

5. Summary

In this paper, we have studied mass spectrum of the $J^P = 1/2^-$ and $3/2^-$ pentaquark antidecuplets initiated by the newly discovered exotic Θ^+ baryon. We have applied the perturbative chiral quark model, where confined valence quarks/antiquarks interact with meson fields according to chiral symmetry requirements and with quantum fluctuations of the gluon field. Guided by experimental preference we selected a specific configuration of the pentaquark system leading to negative parity baryon multiplets: the flavor SU(3) octet and antidecuplet with spin 1/2 and 3/2 for each of these multiplets. The Θ^+ baryon can be considered as a possible member of one of the antidecuplets. Here we payed attention to the antidecuplet only, and evaluated the energy shifts arising from the residual interaction as well as from the current quark masses. The model parameters, *i.e.* the confining potential and the effective quark-gluon coupling, are set up and constrained

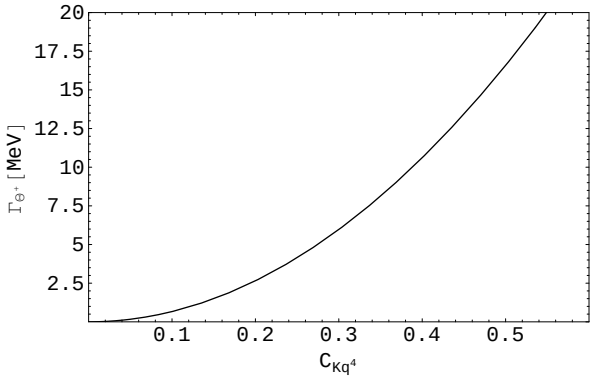

Fig. 6. Width Γ_{Θ^+} as function of c_{Kq^4}.

such as to give a reasonable fit to mass shifts in the octet and decuplet sector of conventional baryons.

Within the model we generate a spin 1/2 antidecuplet which is lighter than for spin 3/2. The observed Θ^+ baryon can be assigned as a member of the spin 1/2 antidecuplet with negative parity. The origin of the splitting between the two multiplets is dominantly traced to the semi-perturbative gluon exchange between the quarks and the antiquark. The size of the splitting is about 185 MeV, which is somewhat smaller when compared to the usual mass difference of the conventional spin 1/2 and 3/2 ground state baryons. This qualitative difference arises from the meson exchange contribution, which shifts the spin 3/2 pentaquark antidecuplet slightly lower with respect to the spin 1/2 one, while the spin 3/2 decuplet of the ground state baryons becomes about 100 MeV heavier relative to the octet. The two spin states are a necessary consequence in most of the pentaquark models, however the splitting between these two are often not studied.

The current quark mass splits the baryon mass inside each antidecuplet according to its strange quark/antiquark content. With the present relativistic quark wave function, the size of the splitting is about 41 MeV between each neighboring row of the isospin multiplets. By this mechanism the bottom member Ξ becomes 123 MeV heavier than the Θ. In addition, the inclusion of the meson cloud gives a considerable mass splitting within each antidecuplet. For instance, we obtain a mass difference of 96 MeV between the spin 1/2 states Θ and Ξ due to meson loops. Our results for SU(3) flavor violation within the multiplets are originally induced by flavor dependent quark masses, which in turn affect the meson masses, and thereby meson loops.

As a final result we have a spin 1/2 Ξ which is 220 MeV heavier than its Θ partner in the multiplet. This value is 30% smaller when compared to the preliminary mass difference of the Θ^+ and Ξ^{--} deduced from data. This result may indicate that the present model is reasonable but probably too simplified in treating con-

finement. We have not studied the decay widths of the pentaquark system yet. The observed narrow decay width of the Θ^+ baryon is a key challenge to explain. At the same time the possible observability of the other members of the multiplet should be worked out in consistency with experimental findings. The issue of the decay patterns of the antidecuplet pentaquark states will be subject of a forthcoming paper.

Finally, we discuss a possible mechanism for a small decay width of the negative-parity Θ^+ baryon. We suggest an existence of relevant effective transition operator which can be generated in the second-order of perturbation theory. Our result is: $\Gamma_{\Theta^+} = 7$ MeV which overestimates the current upper limits for this quantity: $\Gamma_{\Theta^+} = 0.9 \pm 0.3$ MeV [27].

acknowledgments

This work was supported by the Deutsche Forschungsgemeinschaft (DFG) under contracts FA67/25-3 and GRK683. This research is also part of the EU Integrated Infrastructure Initiative Hadron physics project under contract number RII3-CT-2004-506078 and President grant of Russia "Scientific Schools" No. 1743.2003.

Appendix A. Flavor-spin and color-spin matrix elements

In the following we list the flavor-spin and color-spin matrix elements of the antidecuplet pentaquark baryons discussed in the text. Here, the particle label 5 refers to the antiquark while 1 to 4 to the valence quarks. The symbols $\lambda^{(a=1\sim 8)}$ are the flavor Gell-Mann matrices, $\vec{\sigma}$ is the vector of the Pauli spin matrices, and $\vec{\lambda}^C$ is the vector of the color Gell-Mann matrices. In some matrix elements partial contributions of the non-strange quark(n), the strange quark (s), the non-strange ($\bar{n}$) and strange antiquark ($\bar{s}$) are also given.

References

1. T. Nakano *et al.* [LEPS Collaboration], Phys. Rev. Lett. **91**, 012002 (2003) [arXiv:hep-ex/0301020]; V. V. Barmin *et al.* [DIANA Collaboration], Phys. Atom. Nucl. **66**, 1715 (2003) [Yad. Fiz. **66**, 1763 (2003)] [arXiv:hep-ex/0304040]
2. S. Stepanyan *et al.* [CLAS Collaboration], Phys. Rev. Lett. **91**, 252001 (2003) [arXiv:hep-ex/0307018]; J. Barth *et al.* [SAPHIR Collaboration], arXiv:hep-ex/0307083.
3. R. A. Arndt, I. I. Strakovsky and R. L. Workman, arXiv:nucl-th/0311030.
4. C. Alt *et al.* [NA49 Collaboration], Phys. Rev. Lett. **92**, 042003 (2004) [arXiv:hep-ex/0310014]; H. G. Fischer and S. Wenig, Eur. Phys. J. C **37**, 133 (2004) [arXiv:hep-ex/0401014]; J. W. Price, J. Ducote, J. Goetz and B. M. K. Nefkens [CLAS Collaboration], arXiv:nucl-ex/0402006
5. D. Diakonov, V. Petrov and M. V. Polyakov, Z. Phys. A **359**, 305 (1997) [arXiv:hep-ph/9703373].
6. T. D. Cohen, Phys. Lett. B **581**, 175 (2004) [arXiv:hep-ph/0309111].
7. F. J. Llanes-Estrada, E. Oset and V. Mateu, Phys. Rev. C **69**, 055203 (2004) [arXiv:nucl-th/0311020].

8. R. L. Jaffe and F. Wilczek, Phys. Rev. Lett. **91**, 232003 (2003) [arXiv:hep-ph/0307341].
9. M. Karliner and H. J. Lipkin, arXiv:hep-ph/0307243.
10. S. Capstick, P. R. Page and W. Roberts, Phys. Lett. B **570**, 185 (2003) [arXiv:hep-ph/0307019].
11. F. Stancu and D. O. Riska, Phys. Lett. B **575**, 242 (2003) [arXiv:hep-ph/0307010].
12. C. E. Carlson, C. D. Carone, H. J. Kwee and V. Nazaryan, Phys. Lett. B **573**, 101 (2003) [arXiv:hep-ph/0307396].
13. C. E. Carlson, C. D. Carone, H. J. Kwee and V. Nazaryan, Phys. Lett. B **579**, 52 (2004) [arXiv:hep-ph/0310038].
14. B. K. Jennings and K. Maltman, Phys. Rev. D **69**, 094020 (2004) [arXiv:hep-ph/0308286].
15. S. L. Zhu, Phys. Rev. Lett. **91**, 232002 (2003) [arXiv:hep-ph/0307345].
16. J. Sugiyama, T. Doi and M. Oka, Phys. Lett. B **581**, 167 (2004) [arXiv:hep-ph/0309271].
17. S. Sasaki, Phys. Rev. Lett. **93**, 152001 (2004) [arXiv:hep-lat/0310014].
18. V. E. Lyubovitskij, T. Gutsche and A. Faessler, Phys. Rev. C **64**, 065203 (2001) [arXiv:hep-ph/0105043].
19. V. E. Lyubovitskij, T. Gutsche, A. Faessler and E. G. Drukarev, Phys. Rev. D **63**, 054026 (2001) [arXiv:hep-ph/0009341]; V. E. Lyubovitskij, T. Gutsche, A. Faessler and R. Vinh Mau, Phys. Lett. B **520**, 204 (2001) [arXiv:hep-ph/0108134]; Phys. Rev. C **65**, 025202 (2002) [arXiv:hep-ph/0109213]; V. E. Lyubovitskij, P. Wang, T. Gutsche and A. Faessler, Phys. Rev. C **66**, 055204 (2002) [arXiv:hep-ph/0207225]; F. Simkovic, V. E. Lyubovitskij, T. Gutsche, A. Faessler and S. Kovalenko, Phys. Lett. B **544**, 121 (2002) [arXiv:hep-ph/0112277]; K. Pumsa-ard, V. E. Lyubovitskij, T. Gutsche, A. Faessler and S. Cheedket, Phys. Rev. C **68**, 015205 (2003) [arXiv:hep-ph/0304033]; T. Inoue, V. E. Lyubovitskij, T. Gutsche and A. Faessler, Phys. Rev. C **69**, 035207 (2004) [arXiv:hep-ph/0311275]; S. Cheedket, V. E. Lyubovitskij, T. Gutsche, A. Faessler, K. Pumsa-ard and Y. Yan, Eur. Phys. J. A **20**, 317 (2004) [arXiv:hep-ph/0212347]; K. Khosonthongkee, V. E. Lyubovitskij, T. Gutsche, A. Faessler, K. Pumsa-ard, S. Cheedket and Y. Yan, J. Phys. G **30**, 793 (2004) [arXiv:hep-ph/0403119].
20. T. Inoue, V. E. Lyubovitskij, T. Gutsche and A. Faessler, [arXiv:hep-ph/0404051].
21. H. Leutwyler, Nucl. Phys. B **179**, 129 (1981); D. Diakonov and V. Y. Petrov, Nucl. Phys. B **245**, 259 (1984); G. V. Efimov and M. A. Ivanov, *The Quark Confinement Model of Hadrons*, (IOP Publishing, Bristol & Philadelphia, 1993).
22. J. Gasser, M. E. Sainio and A. Svarc, Nucl. Phys. B **307**, 779 (1988).
23. J. Gasser and H. Leutwyler, Phys. Rept. **87**, 77 (1982).
24. P. Maris and P. C. Tandy, Phys. Rev. C **60**, 055214 (1999) [arXiv:nucl-th/9905056]; C. D. Roberts and S. M. Schmidt, Prog. Part. Nucl. Phys. **45**, S1 (2000) [arXiv:nucl-th/0005064].
25. B. G. Wybourne, arXiv:hep-ph/0307170.
26. F. E. Close, AIP Conf. Proc. **717**, 919 (2004) [arXiv:hep-ph/0311087].
27. R. N. Cahn and G. H. Trilling, Phys. Rev. D **69** 011501 (2004) [arXiv:hep-ph/0311245].
28. M. Eidemuller, F. S. Navarra, M. Nielsen and R. R. da Silva, arXiv:hep-ph/0503193.
29. D. Diakonov and V. Petrov, arXiv:hep-ph/0505201.
30. Z. G. Wang, W. M. Yang and S. L. Wan, arXiv:hep-ph/0504151.

Table 4. Matrix element $\langle 1^C, \bar{1}0^F, \frac{1}{2}^S(\frac{3}{2}^S)|\sum_{i<j}^{4}\sum_a \lambda_i^{(a)}\lambda_j^{(a)}\vec{\sigma}_i\cdot\vec{\sigma}_j\,|1^C, \bar{1}0^F, \frac{1}{2}^S(\frac{3}{2}^S)\rangle$ in units of 1/27.

	$a=1\sim3$	$a=4\sim7$	$a=8$			
	nn	ns	nn	ns	ss	total
Θ	270	0	−18	0	0	−18
N	180	72	−12	12	0	0
Σ	93	132	−5	28	4	27
Ξ	9	180	3	48	12	63

Table 5. Matrix element $\langle 1^C, \bar{1}0^F, \frac{1}{2}^S|\sum_{i=1}^{4}\sum_a \lambda_i^{(a)}\lambda_5^{(a)}\,\vec{\sigma}_i\cdot\vec{\sigma}_5\,|1^C, \bar{1}0^F, \frac{1}{2}^S\rangle$ in units of 1/9.

	$a=1\sim3$	$a=4\sim7$	$a=8$				
	$n\bar{n}$	$n\bar{n}(s\bar{s})$	$n\bar{n}$	$n\bar{s}$	$s\bar{n}$	$s\bar{s}$	total
Θ	0	0	0	−24	0	0	−24
N	0	−24	4	−12	0	8	0
Σ	−6	−24	6	−4	−4	8	6
Ξ	−18	0	6	0	−12	0	−6

Table 6. Matrix element $\langle 1^C, \bar{1}0^F, \frac{3}{2}^S|\sum_{i=1}^{4}\sum_a \lambda_i^{(a)}\lambda_5^{(a)}\,\vec{\sigma}_i\cdot\vec{\sigma}_5\,|1^C, \bar{1}0^F, \frac{3}{2}^S\rangle$ in units of 1/9.

	$a=1\sim3$	$a=4\sim7$	$a=8$				
	$n\bar{n}$	$n\bar{n}(s\bar{s})$	$n\bar{n}$	$n\bar{s}$	$s\bar{n}$	$s\bar{s}$	total
Θ	0	0	0	12	0	0	12
N	0	12	−2	6	0	−4	0
Σ	3	12	−3	2	2	−4	−3
Ξ	9	0	−3	0	6	0	3

Table 7. Matrix element $\langle 1^C, \bar{1}0^F, \frac{1}{2}^S(\frac{3}{2}^S)|\sum_{i=1}^{4}\sum_a \lambda_i^{(a)}\lambda_i^{(a)}\,|1^C, \bar{1}0^F, \frac{1}{2}^S(\frac{3}{2}^S)\rangle$ in units of 1/9.

	$a=1\sim3$	$a=4\sim7$			$a=8$		
	n	n	s	total	n	s	total
Θ	108	72	0	72	12	0	12
N	90	60	24	84	10	8	18
Σ	72	48	48	96	8	16	24
Ξ	54	36	72	108	6	24	30

Table 8. Matrix element $\langle 1^C, \bar{1}0^F, \frac{1}{2}^S(\frac{3}{2}^S)| \sum_a \lambda_5^{(a)}\lambda_5^{(a)} \ |1^C, \bar{1}0^F, \frac{1}{2}^S(\frac{3}{2}^S)\rangle$ in units of 1/9.

	$a=1\sim 3$	$a=4\sim 7$			$a=8$		
	$\bar{n}$	$\bar{n}$	$\bar{s}$	total	$\bar{n}$	$\bar{s}$	total
Θ	0	0	36	36	0	12	12
N	9	6	24	30	1	8	9
Σ	18	12	12	24	2	4	6
Ξ	27	18	0	18	3	0	3

Table 9. Matrix element $\langle 1^C, \bar{1}0^F, \frac{1}{2}^S(\frac{3}{2}^S)| \sum_{i<j}^4 \vec{\lambda}_i^C \cdot \vec{\lambda}_j^C \, \vec{\sigma}_i \cdot \vec{\sigma}_j \ |1^C, \bar{1}0^F, \frac{1}{2}^S(\frac{3}{2}^S)\rangle$ in units of 1/27.

	nn	ns	ss	total
Θ	144	0	0	144
N	96	48	0	144
Σ	22	148	-26	144
Ξ	-78	300	-78	144

Table 10. Matrix element $\langle 1^C, \bar{1}0^F, \frac{1}{2}^S| \sum_{i=1}^4 \vec{\lambda}_i^C \cdot \vec{\lambda}_5^C \, \vec{\sigma}_i \cdot \vec{\sigma}_5 \ |1^C, \bar{1}0^F, \frac{1}{2}^S\rangle$ in units of 1/9.

	$n\bar{n}$	$n\bar{s}$	$s\bar{n}$	$s\bar{s}$	total
Θ	0	120	0	0	120
N	40	60	0	20	120
Σ	60	20	20	20	120
Ξ	60	0	60	0	120

Table 11. Matrix element $\langle 1^C, \bar{1}0^F, \frac{3}{2}^S| \sum_{i=1}^4 \vec{\lambda}_i^C \cdot \vec{\lambda}_5^C \, \vec{\sigma}_i \cdot \vec{\sigma}_5 \ |1^C, \bar{1}0^F, \frac{3}{2}^S\rangle$ in units of 1/9.

	$n\bar{n}$	$n\bar{s}$	$s\bar{n}$	$s\bar{s}$	total
Θ	0	-60	0	0	-60
N	-20	-30	0	-10	-60
Σ	-30	-10	-10	-10	-60
Ξ	-30	0	-30	0	-60

Table 12. Matrix element $\langle 1^C, \bar{1}0^F, \frac{1}{2}^S(\frac{3}{2}^S)| \sum_{i<j}^{4} \vec{\lambda}_i^C \cdot \vec{\lambda}_j^C \ |1^C, \bar{1}0^F, \frac{1}{2}^S(\frac{3}{2}^S)\rangle$ in units of 1/9.

	nn	ns	ss	total
Θ	-72	0	0	-72
N	-48	-24	0	-72
Σ	-30	-36	-6	-72
Ξ	-18	-36	-18	-72

Table 13. Matrix element $\langle 1^C, \bar{1}0^F, \frac{1}{2}^S(\frac{3}{2}^S)| \sum_{i=1}^{4} \vec{\lambda}_i^C \cdot \vec{\lambda}_5^C \ |1^C, \bar{1}0^F, \frac{1}{2}^S(\frac{3}{2}^S)\rangle$ in units of 1/9.

	$n\bar{n}$	$n\bar{s}$	$s\bar{n}$	$s\bar{s}$	total
Θ	0	-48	0	0	-48
N	-16	-24	0	-8	-48
Σ	-24	-8	-8	-8	-48
Ξ	-24	0	-24	0	-48

Table 14. Matrix element $\langle 1^C, \bar{1}0^F, \frac{1}{2}^S(\frac{3}{2}^S)| \sum_{i=1}^{5} \vec{\lambda}_i^C \cdot \vec{\lambda}_i^C \ |1^C, \bar{1}0^F, \frac{1}{2}^S(\frac{3}{2}^S)\rangle$ in units of 16/3.

	n	s	$\bar{n}$	$\bar{s}$	total
Θ	4	0	0	1	5
N	$\frac{10}{3}$	$\frac{2}{3}$	$\frac{1}{3}$	$\frac{2}{3}$	5
Σ	$\frac{8}{3}$	$\frac{4}{3}$	$\frac{2}{3}$	$\frac{1}{3}$	5
Ξ	2	2	1	0	5